

File ID uvapub:46433
Filename 210997y.pdf
Version unknown

SOURCE (OR PART OF THE FOLLOWING SOURCE):

Type article
Title Raman Fingerprint of Orientational Freezing in Mixed Molecular-Crystals
Author(s) W. Joosen, H. Fleurent, C. Bostoen, D. Schoemaker, S. Haussuhl
Faculty UvA: Universiteitsbibliotheek
Year 1991

FULL BIBLIOGRAPHIC DETAILS:

<http://hdl.handle.net/11245/1.426561>

Copyright

It is not permitted to download or to forward/distribute the text or part of it without the consent of the author(s) and/or copyright holder(s), other than for strictly personal, individual use, unless the work is under an open content licence (like Creative Commons).

Raman fingerprint of orientational freezing in mixed molecular crystals

W. Joosen*

*Foundation for Fundamental Research on Matter (FOM)-Institute for Atomic and Molecular Physics,
1098 SJ Amsterdam, The Netherlands*

H. Fleurent

Natuurkundig Laboratorium, Universiteit van Amsterdam, 1018 XE Amsterdam, The Netherlands

C. Bostoen and D. Schoemaker

Physics Department, University of Antwerp, B-2610 Wilrijk-Antwerp, Belgium

S. Haussühl

Institut für Kristallographie, University of Köln, 5000 Köln, Federal Republic of Germany

(Received 10 September 1990)

The internal modes of the CN^- , NO_2^- , and NH_4^+ ions in mixed molecular alkali halides exhibit concentration-dependent anomalies in their polarized Raman spectra, reflecting dipolar or quadrupolar freezing. At low temperatures the cubic degeneracy of the polarized intensities is lifted by an ordering effect with the same symmetry as existing phases of the pure molecular crystal.

The polarized Raman spectra of KI and KBr, containing large concentrations of NO_2^- molecular ions, exhibit unusual polarization properties at low temperatures: Particular polarized Raman intensities, which are equal for isolated molecules, become unequal at higher dopant levels.¹ As little information on concentration-dependent phenomena in NO_2^- -doped alkali halides is available, we extended the Raman data to $\text{K}(\text{CN})_x\text{Br}_{1-x}$, which has a well-established (x, T) phase diagram,² and also to $\text{K}_{1-x}(\text{NH}_4)_x\text{I}$. In this Rapid Communication the universal character of these polarized Raman intensity variations in mixed molecular crystals is demonstrated.

$\text{K}(\text{CN})_x\text{Br}_{1-x}$ has become a model system for the investigation of collective phenomena such as ferroelastic and ferroelectric ordering, and orientational freezing, because it is possible to study the gradually changing crystal properties over the complete cyanide concentration range $0 \leq x \leq 1$. Above the critical concentration ($x_c = 0.6$) ferroelastic deformations, originating from the coupling between the translational modes of the center-of-mass lattice and the quadrupolar rotational motion of the CN^- molecular ion,³ induce a transition into a low-temperature noncubic phase with long-range orientational order.⁴ Below x_c , the inhomogeneous strain fields, due to the misfit of the Br^- ions, suppress the ferroelastic order⁵ and trigger a transition into an orientational glass state. This state with overall cubic symmetry is characterized by frozen, orientational disorder.⁶

The phase diagram of $\text{K}(\text{CN})_x\text{Br}_{1-x}$ has been determined with different experimental techniques.⁷⁻⁹ For a particular range of cyanide concentrations ($0.2 < x < 0.57$) the orientational glass state was shown to exhibit the same properties as structurally disordered "real" glasses like, e.g., vitreous silica.¹⁰⁻¹² This resemblance has increased the appeal to studying molecular interactions in mixed molecular crystals.

Only a few Raman scattering experiments have focused on collective phenomena in heavily doped alkali halides. Data for isolated molecular defects and pure molecular crystals were reported for several different molecules (NO_2^- , CN^- , NO_3^-).^{1,7} Only $\text{K}(\text{CN})_x\text{Cl}_{1-x}$ and $\text{K}(\text{CN})_x\text{Br}_{1-x}$ were studied over a large concentration range.¹³ Recently, the increasing Raman linewidth of the CN^- stretching mode in $\text{K}(\text{CN})_x\text{Br}_{1-x}$ for decreasing temperatures was correlated with frozen-in orientational disorder.¹⁴ The polarization properties of the Raman scattering were up until now only investigated in the I_{yy} and I_{yz} scattering geometries,¹⁵ discarding this way essential information. For the 5 mol % doped KBr:CN⁻ sample, studied in this paper, clustering and the presence of ferroelastic anomalies were evidenced in thermal conductivity, specific heat,¹⁰ Brillouin,¹⁵ ultrasonic,¹⁶ and inelastic neutron-scattering measurements.¹⁷

The Raman measurements were performed on the intramolecular vibrations in $\text{K}(\text{CN})_{0.05}\text{Br}_{0.95}$, $\text{K}(\text{NO}_2)_{0.018}\text{I}_{0.982}$, and $\text{K}_{0.57}(\text{NH}_4)_{0.43}\text{I}$. The polarized spectra of the CN^- stretching vibration (2077 cm^{-1}) were recorded under 488-nm excitation (120 mW) in a {100}-cut sample in the temperature range between 9 and 60 K. The temperature dependence of the depolarized intensities I_{yz} , I_{xz} , and I_{xy} is depicted in Fig. 1(a). The three distinct branches, detected at 9 K, gradually approach each other and coincide above 40 K. The splitting pattern is well reproducible, i.e., $I_{xz} \leq I_{yz} \leq I_{xy}$. The depolarized intensities of the internal modes of NO_2^- in $\text{K}(\text{NO}_2)_{0.018}\text{I}_{0.982}$ and of NH_4^+ in $\text{K}_{0.57}(\text{NH}_4)_{0.43}\text{I}$ exhibit comparable temperature effects, as shown in Figs. 1(b) and 1(c). The splitting temperature is 90 K for KI: NO_2^- and 60 K for KI: NH_4^+ . For these two cases the cubic degeneracy of the depolarized intensities is lifted such that $I_{yz} \leq I_{xz} < I_{xy}$.

A nonsystematic, relative variation of 10% in the ratio

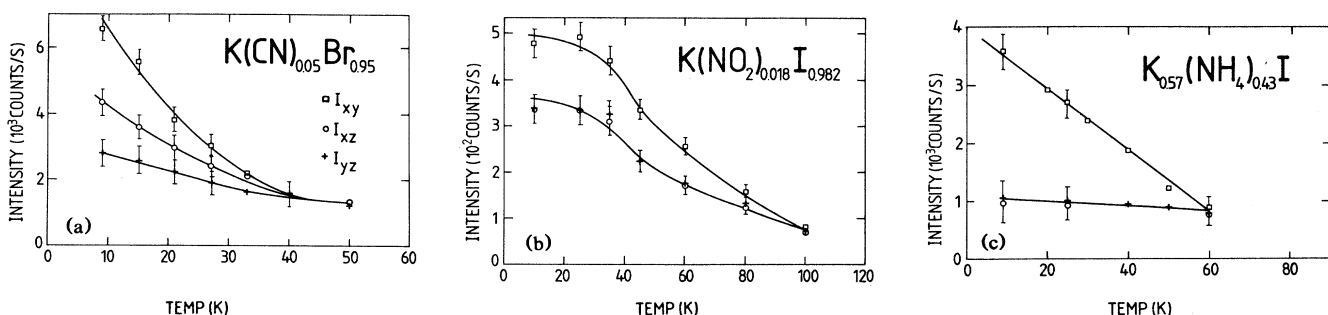


FIG. 1. Temperature dependence of the depolarized intensities I_{yz} , I_{xz} , and I_{xy} of (a) the A_1 stretching mode of CN^- in $\text{K}(\text{CN})_{0.05}\text{Br}_{0.95}$, (b) the $v_2(A_1)$ mode of NO_2^- in $\text{K}(\text{NO}_2)_{0.018}\text{I}_{0.982}$, and (c) the $v_1(A_1)$ mode of $\text{K}_{0.57}(\text{NH}_4)_{0.43}\text{I}$. Squares, I_{xy} ; crosses, I_{yz} ; and circles, I_{xz} . Peak heights are presented, because the widths of the three peaks are equal at all temperatures. The non-monotonic intensity decrease for $\text{K}(\text{NO}_2)_{0.018}\text{I}_{0.982}$ is mainly due to peak broadening. The solid lines are guides to the eye.

I_{xy}/I_{yy} is detected when the location of the scattering volume is changed in the CN^- and NO_2^- -doped samples. Only in the 43% doped KI:NH_4^+ sample a systematic increase of this ratio is observed, when shifting the interaction volume from the center to the crystal edges. We observed a 15-K hysteresis effect in $\text{K}_{0.57}(\text{NH}_4)_{0.43}\text{I}$ between 25 and 50 K. The 0.03-mol% doped KI:NO_2^- sample was accurately oriented¹ and for all internal modes as well as the low-frequency region the usual cubic degeneracy for isolated defects was observed, i.e., $I_{xz} = I_{xy} = I_{yz}$. Horizontal translation of the cryostat permits polarized Raman measurements with equal accuracy in the 1.8-mol% doped sample. We found that at low temperatures the cubic degeneracy was broken [Fig. 1(b)].

For randomly distributed defects in cubic lattices, the intensity equalities $I_{xy} = I_{xz} = I_{yz}$ are expected to occur when the crystal axes are properly aligned with respect to the incident polarization directions.¹⁸ Therefore, only the I_{yy} and I_{yz} intensities are usually determined. The breakdown of the above intensity equalities in a cubic lattice generally demonstrates a nonrandom distribution of defects. Such a distribution can be attained by preferential optical bleaching or by applying an external electric or strain field. In the weak-field limit, the internal modes for different molecular orientations are characterized by an identical Raman tensor, apart from a unitary transformation, representing the rotation from one direction to another. This approximation can probably not be applied for higher concentrations, at which strong local (strain or electric) fields due to the molecular interactions will perturb the Raman tensor elements in a way different from site to site.

In the assumption that the Raman tensor elements are rather insensitive for these inhomogeneities, the present data reveal a nonrandom distribution of molecular ions, i.e., with different population numbers for the orientationally degenerate directions. One has to use the calculated polarized intensities for nonrandomly oriented defects¹⁸ to find the symmetry of the ordering effect.

As similar polarized Raman anomalies were observed for different internal modes, characterized by different irreducible representations, a low site symmetry is re-

trieved. This is consistent with the common description of the orientational glass state, which assumes an angular distribution of the molecular orientations around the average potential minima. Assuming six independent components for the Raman tensor of the intramolecular vibration in such a low-symmetric (C_1) configuration, the low-temperature Raman data can be interpreted in terms of an orientating operator (ordering effect),¹⁸ which corresponds to the symmetry of the local strain field and thus of the nonrandom distribution in the scattering volume. For the NO_2^- -doped samples we deduce an ordering effect with $C_3[111]$ or $D_3[111]$ symmetry in KBr , and with $D_2[011]$ symmetry in KI . The polarized Raman intensities in KI:NH_4^+ reflect a tetragonal preferential distribution ($C_4[001]$ symmetry) and those in KBr:CN^- correspond to an orthorhombic $C_2[100]$ or $D_2[100]$ orientating operator.

The pure molecular crystal KNO_2 , NH_4I , and KCN show structural phase transitions from a high-temperature face-centered cubic structure into phases with rhombohedral, tetragonal, and orthorhombic symmetry, respectively: The ordering effect, which breaks down the cubic degeneracy of the depolarized intensities in the mixed systems, has the same symmetry as these high-temperature phases.

The freezing temperature T_f , indicating the transition into an orientational glass state, is dependent on the frequency of the experimental probe. T_f exhibits to a large extent an Arrhenius law behavior on the probe frequency.¹⁹ Higher probe frequencies and higher concentrations yield a higher value for the observed freezing temperature. A lower bound for T_f in the $\text{K}(\text{CN})_{0.05}\text{Br}_{0.95}$ sample can be estimated from ultrasonic data (MHz) for a 3.5% doped KBr:CN^- sample, yielding $T_f = 16.5$ K (Ref. 20). A possible upper bound is derived from inelastic neutron-scattering data (1–4 THz) on $x = 0.16$ samples, giving 55 K for T_f (Ref. 21). A lack of systematic T_f data for the (v, x) matrix inhibits a more accurate estimate of the freezing temperature. The present Raman data of $\text{K}(\text{CN})_{0.05}\text{Br}_{0.95}$ were measured under visible light excitation (600 THz) and yield a splitting temperature of 40 K of the depolarized intensities. This is a reasonable value of T_f on the time scale of the Raman scattering probe.

The observation of similar effects in other crystals with higher doping levels [see Figs. 1(b) and 1(c)] shows the general character of the symmetry breaking in the polarized Raman spectra.

Collective orientational freezing can be governed by (i) direct interactions between the electrostatic dipoles, e.g., OH⁻ in KCl (Ref. 22) or quadrupoles, e.g., N₂/Ar mixtures,²³ or (ii) indirect, lattice mediated interactions, e.g., in K(CN)_xBr_{1-x}. In the latter case the competition between translation-rotation and random strain-rotation coupling determines the phase diagram.⁵ The intermolecular interactions in the NO₂⁻-doped alkali halides may be of either kind. The isolated NO₂⁻ molecular ion in KBr and KI is characterized by a different orientation (C_{3v} and C_{2v} site symmetry, respectively),¹ a different lattice position (on-center and off-center, respectively) and a different electric dipole moment (0.21 and 0.97 D, respectively). Therefore, the interaction mechanism will be host dependent, despite the common high concentration limit KNO₂. For NO₂⁻ in KBr it is possible that the quasifree rotation of the molecule about its O-O axis induces a quadrupolar deformation and lattice-mediated interactions similar to those detected in K(CN)_xBr_{1-x}.

A discovery is the *non-tetrahedral* behavior of the polarized Raman data of NH₄⁺ in KI, even at concentrations as low as 0.5 mol %. This shows that the orientational freezing in this system is probably not related with octopole-octopole interactions, which usually govern the correlation effects among tetrahedral molecular ions. To our knowledge, this is the first case of symmetry breaking for a tetrahedral molecular ion in alkali halides. The observation is in agreement with recent dielectric measurements on K_{0.57}(NH₄)_{0.43}I (Ref. 24). It also supports the inelastic neutron-scattering data,²⁵ which show for increasing NH₄⁺ concentration a broad distribution of tunneling lines and an anomalously strong quasielastic peak, which cannot be explained by these short-range interactions only.

The Raman spectra of the internal bending and stretching region of a 0.5-mol % doped KI:NH₄⁺ sample are presented in Fig. 2. The polarized Raman intensities were analyzed with the behavior-type (BT) method for randomly oriented defects in cubic crystals.¹⁸ An overview of various applications of this method was given recently.²⁶

Tetrahedral molecular ions (point group T_d) possess four intramolecular vibrations, i.e., $v_1(A_1)$, $v_2(E)$, $v_3(T_2)$, and $v_4(T_2)$, all of which are Raman active (Fig. 2). The strong intensity of the overtones and/or combination modes $2v_4$ and v_2+v_4 ($2v_2$) is due to a Fermi resonance with the v_3 (v_1) mode. A substitutional tetrahedral molecular ion may accommodate in an fcc alkali halide with C_{3v} , C_{2v} , D_{2d} , or T_d symmetry. In the latter case four equivalent N-H bonds point along the $\langle 111 \rangle$ directions of the cubic lattice, corresponding to specific sets of intensity parameter (IP) ratios, i.e., BT 13 ($s/q=0$, $r/q=1$), BT 14 ($s/q=0$, $r/q=-0.5$), and BT 15 ($s\neq0$, $r=q=0$) for the A_1 , E , and T_2 modes, respectively.

The observed BT's are indicated in Fig. 2. None of the internal vibrations exhibits the polarized intensities, expected for $T_d:T_2$ modes, which unquestionably points at symmetry lowering. Instead, BT 14 is detected for both v_3

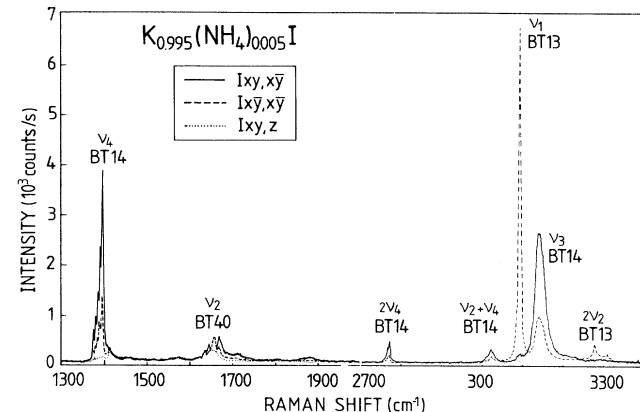


FIG. 2. Polarized Raman spectra of the bending and stretching region of NH₄⁺, recorded in a {110}-polished K_{0.995}(NH₄)_{0.005}I sample. The fundamentals, overtones, and combination modes are indicated, together with their observed BT. Temperature 9 K and resolution 2.5 cm⁻¹.

and v_4 , whereas v_1 possesses a BT 13 and v_2 a BT 40 ($s/q\neq0$, $r/q=-0.5$). The splitting of the threefold degenerate T_2 modes, associated with a nontetrahedral symmetry, has been detected in ir absorption measurements,²⁷ but is not observable in the Raman data. This is probably related with different intrinsic Raman cross sections of the components. The combination of observed BT's 13, 14, and 40 is consistent with a C_{3v} symmetry, when accidental degeneracy of the s/q IP in v_1 , v_3 , and v_4 is taken into account: a nonzero s/q ratio, combined with the observed $r/q=1$ and $r/q=-0.5$, corresponds to a $C_{3v}:A_1$ (BT 39) and a $C_{3v}:E$ (BT 40) mode, respectively. The zero $I_{xy,z}$ intensity (or, equivalently, the zero s IP) of v_4 and the stretching modes between 2600 and 3200 cm⁻¹ is probably caused by the large polarizability of the surrounding iodine ions.²⁸ In the fcc high-temperature phases of NH₄I and NH₄Cl very different s/q ratios were observed, i.e., 1.5% and 38%, respectively.²⁹ Therefore, the polarized Raman data of the fundamental, overtone, and combination modes are compatible with C_{3v} symmetry. This supports Ozaki's calculations, which explain the tunneling level structure for KBr:NH₄⁺ in terms of a C_{3v} potential.³⁰ The nonequivalency of the hydrogens induces an electric dipole moment and the interactions among these dipoles can explain the strong concentration dependence of the neutron-scattering data in K_{1-x}(NH₄)_xI.²⁵

It was argued that a nonrandom population distribution within the cubic lattice environment is compatible with the present Raman observations. The presence of *small domains* is not excluded, but they must be smaller than the wavelength of the exciting laser beam (500 nm) to be compatible with the optical transparency of the crystal. The degeneracy of the depolarized intensities would also be lifted in a noncubic structure. A *noncubic glass* state was previously observed for other systems by x-ray diffraction experiments.^{23,31} The splitting patterns observed for the positions of the Bragg reflections as a function of temperature are similar to those of Fig. 1. However, in K(CN)_xBr_{1-x} the diffraction data during the freez-

ing process show Bragg spots, which are still centered at the fcc reciprocal lattice points. The diffuseness of the spots reflects a breakdown of the cubic arrangement of the center-of-mass lattice on a local scale, whereas the averaged symmetry over larger distances is still cubic.³² An interpretation of the present Raman data in terms of a noncubic unit cell would imply a different fingerprint for the interaction effects in light scattering with respect to all other techniques.

The Raman process probes the distortion of the electron cloud due to anisotropic interactions on a time scale, fast in comparison with all the other experimental techniques. It probably also probes rapid fluctuations of the derived polarizability, which do not follow adiabatically the molecular vibrations. These fluctuations reflect the inhomogeneous interactions, which for decreasing temperature drive the freezing of both the rotational and translational degrees of freedom,⁶ and are more sensitive to the interactions with other molecular ions than to the local molecular potential. The "electronic freezing" of these fluctuations may persist after the orientational freezing.

It is concluded that the concentration- and tem-

perature-dependent anomalies in the polarized Raman intensities of the intramolecular modes of highly doped mixed molecular crystals possess a universal character and reflect orientational freezing. The low-temperature intensity splittings are related to partial ordering, possibly into small domains or to dynamical fluctuations of the electronic wave function by inhomogeneous strains. An important specific result is the symmetry breaking of the isolated NH₄⁺ ion in KI, indicating that dipolar interactions are important at higher NH₄⁺ concentrations. Consequently, the mixed crystal K_{1-x}(NH₄)_xI can be considered as a model system for dipolar glassy behavior,²⁷ complementary to the well-established quadrupolar K(CN)_xBr_{1-x} glass.

We thank M. Meissner for sending us a K(CN)_{0.05}Br_{0.95} sample. Interesting discussions with K. H. Michel are gratefully acknowledged. This work was supported by NFWO (Nationaal Fonds voor Wetenschappelijk Onderzoek) and IIKW (Interuniversitair Instituut voor Kernwetenschappen) to which the authors are greatly indebted.

*Present address: Centre d' Etudes Nucléaires de Saclay, Service de Physique des Atomes et des Surfaces, F-91191 Gif-sur-Yvette, France.

¹H. Fleuret, W. Joosen, and D. Schoemaker, Phys. Rev. B **41**, 7774 (1990).

²K. Knorr and A. Loidl, Phys. Rev. B **31**, 5387 (1985).

³K. H. Michel and J. Naudts, Phys. Rev. Lett. **39**, 212 (1977).

⁴K. Knorr and A. Loidl, Phys. Rev. B **31**, 5387 (1985).

⁵K. H. Michel, Phys. Rev. Lett. **57**, 2188 (1986); Phys. Rev. B **35**, 1405 (1987).

⁶K. H. Michel and J. M. Rowe, Phys. Rev. B **22**, 1417 (1980).

⁷F. Lüty, in *Defects in Insulating Crystals*, edited by V. M. Tuchkevitch and K. K. Shvarts (Springer, Berlin, 1981).

⁸J. J. De Yoreo *et al.*, Phys. Rev. B **34**, 8828 (1986).

⁹K. Knorr, Phys. Scr. **T19**, 531 (1987).

¹⁰J. J. De Yoreo *et al.*, Phys. Rev. Lett. **51**, 1050 (1983).

¹¹J. F. Berret *et al.*, Phys. Rev. Lett. **55**, 2013 (1985).

¹²S. Bhattacharya *et al.*, Phys. Rev. Lett. **48**, 1267 (1982).

¹³D. Durand and F. Lüty, Ferroelectrics **16**, 205 (1977).

¹⁴J. F. Berret, J. L. Sauvajol, and G. Cohen-Solal, Europhys. Lett. **13**, 273 (1990).

¹⁵J. J. Vanderwal, Z. Hu, and D. Walton, Phys. Rev. B **33**, 5782 (1986).

¹⁶R. Feile, A. Loidl, and K. Knorr, Phys. Rev. B **26**, 6875 (1982).

¹⁷A. Loidl *et al.*, Phys. Rev. B **29**, 6052 (1984).

¹⁸J. F. Zhou, E. Goovaerts, and D. Schoemaker, Phys. Rev. B **29**, 5509 (1984).

¹⁹U. G. Volkmann *et al.*, Phys. Rev. Lett. **56**, 1716 (1986).

²⁰R. Feile, A. Loidl, and K. Knorr, Phys. Rev. B **26**, 6875 (1982).

²¹A. Loidl *et al.*, Phys. Rev. B **29**, 6052 (1984).

²²W. Känzig, W. R. Hart, Jr., and S. Roberts, Phys. Rev. Lett. **13**, 543 (1965).

²³H. Klee, H. O. Carmesin, and K. Knorr, Phys. Rev. Lett. **61**, 1855 (1988).

²⁴I. Fehst *et al.*, Phys. Rev. Lett. **64**, 3139 (1990).

²⁵C. Bostoen, G. Coddens, and W. Wegener, J. Chem. Phys. **91**, 6337 (1989).

²⁶W. Joosen and D. Schoemaker, J. Phys. Chem. Solids **51**, 821 (1990).

²⁷W. Vedder and D. F. Hornig, J. Chem. Phys. **35**, 1560 (1961).

²⁸R. Pick (private communication).

²⁹M. Couzi, J. B. Sokoloff, and C. H. Perry, J. Chem. Phys. **58**, 2965 (1973).

³⁰Y. Ozaki, K. Maki, K. Okada, and J. A. Morrison, J. Phys. Soc. Jpn. **54**, 2595 (1985); Y. Ozaki, *ibid.* **56**, 1017 (1987).

³¹S. Elschner, K. Knorr, and A. Loidl, Z. Phys. B **61**, 209 (1985).

³²K. Knorr and A. Loidl, Phys. Rev. Lett. **57**, 460 (1986); A. Loidl *et al.*, Phys. Rev. B **37**, 389 (1988).